Proceedings of the ASME 2010 Dynamic Systems and Control Conference
DSCC2010
September 12-15, 2010, Cambridge, Massachusetts, USA

DSCC2010-4033

MODEL PREDICTIVE CONTROL OF A DISTRIBUTED-PARAMETER PROCESS EMPLOYING A MOVING RADIANT ACTUATOR

Fan Zeng
Beshah Ayalew
Department of Mechanical Engineering
Clemson University–International Center for Automotive Research
Greenville, SC, 29607
fzeng@clemson.edu, beshah@clemson.edu

ABSTRACT

Many industrial processes employ radiation-based actuators with two or more manipulated variables. Moving radiant actuators, in particular, act on a distributed parameter process where the velocity of the actuator is an additional manipulated variable with its own constraints. In this paper, a model predictive control (MPC) scheme is developed for a distributed-parameter process employing such a moving radiant actuator. The designed MPC controller uses an online optimization approach to determine both the radiant intensity and velocity of the moving actuator based on a linearized process model and a distributed state/parameter estimator. A particular source-model reduction that enables the approach is outlined. The proposed strategy is then demonstrated for a radiative curing process considering different control scenarios with the objective of achieving desired cure level uniformity and minimizing process energy use.

INTRODUCTION

Recently, radiation-based technologies, such as ultraviolet (UV) curing and infrared (IR) drying, are finding increasing applications in various industrial processes once dominated by traditional convection-based methods. With their improved energy efficiency and reduced use of volatile organic compounds (VOCs), these radiation-based processes can help establish new resource-economical and environment-friendly manufacturing modalities for modern industry [1, 2]. However, in trying to accomplish good product quality for spatially large objects, such as automobile bodies and aircraft structures, installations of numerous radiative sources (e.g. an array of UV-lamps) may be required. This increases the equipment cost and compromises the energy use with the radiative processes [3]. An alternative approach is to use moving radiative devices [6, 8]. Practically, the radiative sources can be installed on the end effectors of robotic manipulators so that they can move around the targets [4, 5]. Compared to the fixed-source configuration, this moving source approach not only reduces the number of radiative sources used but also provides flexibility for conducting various tasks, including covering complex target geometries by using the same hardware configuration.

In order to ensure the desired process quality, however, the moving source/radiant actuator must be carefully controlled to distribute the energy over the target evenly and properly. The problem is one of a distributed parameter process control using mobile actuators. The early study of such problems was conducted by Butkovskii and co-workers [6]. They proposed the concept of mobile control and developed a maximum principle for distributed parameter systems. In further research, Demetriou et. al, developed some optimal strategies to guide and schedule the moving actuator between a priori selected set of locations [7-9]. In a similar problem, Jones and co-workers designed a time-varying H_2 controller to regulate the surface temperature profile for a spray deposition process by adjusting the feed rate of a moving spray gun [10]. These theories and methods either address the framework for such control problems or provide solutions for some particular applications, but most of them seldom discuss the coordination between multiple manipulated variables of the moving actuator.

The present work is motivated by our prior research on the development of closed-loop control approaches for a robotic UV paint curing process [11-13], where the UV source on a robotic end-effector constitutes the moving actuator. The temperature distribution over the target surface captured by IR cameras has been used either directly for simple output feedback control design [11, 12] or integrated into a

state/parameter estimation scheme to determine the cure-status for feedback purposes [13].

The distributed parameter processes cited above typically include the option of manipulating two or more variables (e.g. intensity and velocity) of the moving actuator. Model predictive control (MPC) provides a framework for the optimal coordination of these variables and for taking into account actuator limitations. Some MPC frameworks for distributed parameter processes have been proposed and discussed in [14-16], but most of them focus on processes involving a large centrally fixed actuator or multiple actuators distributed around the object, with the problem then reduced to determining switching policies. Research on formulating MPC strategies for processes that use moving radiant actuators is rarely reported. In this paper, we detail our first work on formulating an MPC control scheme for the distributed parameter process of UV curing employing a moving radiant source. We outline a source-model reduction to enable linearization while retaining the main features of the radiant source. The MPC strategy will incorporate the distributed state/parameter estimator discussed in our previous work [13]. A simulation study is also conducted to demonstrate the proposed MPC scheme.

The rest of this paper is organized as follows. The next section describes the model development and linearization for the UV curing process. This is followed by a section that details the formulation of the MPC strategy. Then, simulation results implementing the MPC strategy are presented and discussed. The last section summarizes the conclusions of this work and addresses future research topics.

MODEL DEVELOPMENT AND LINEARIZATION

The first simplification in modeling the curing process, involves simplifying the path followed by the moving radiative actuator, which in general, can be complex. Here, the curing process is considered as a 1D scanning problem. The moving actuator is modeled as a single point source, since it is small compared to the target. The source is assumed to move parallel to the target. A nonlinear continuous time model of the curing process is developed first based on these assumptions, and then the linear and discrete forms of the process model are derived. Due to the difficulties in measuring the process state directly for this particular case, the control scheme will incorporate the state/parameter estimator outlined elsewhere [13].

Modeling of the UV Curing Process

The general mechanism of the UV curing process has been studied and discussed in [17]. It can be characterized by three fundamental phases: irradiation, photo-initiated polymerization and thermal evolution within the UV curable paint film. The distributed-parameter form of this process is adapted as follows:

$$I(x,t) = \eta(x)\frac{\varphi(t)d_0^2}{\pi\left\{\left[x_a(t)-x\right]^2 + d_0^2\right\}^2} \tag{1}$$

$$\frac{dM(x,t)}{dt} = \kappa M(x,t)u(x,t) \tag{2}$$

$$\rho c\frac{dT(x,t)}{dt} = \lambda\nabla\left[\nabla T(x,t)\right] + R_p\Delta H - h\left[T(x,t)-T_\infty\right] \tag{3}$$

Here, x and t denote the spatial coordinate and time, respectively. Eq. (1) describes the UV irradiation between the moving actuator and the target. The UV irradiation distribution on the target is influenced by the absorption coefficient ($\eta(x)$), the intensity ($\varphi(t)$) and position ($x_a(t)$) of the UV source, and the normal distance (d_0) between the source and target. The polymerization induced by the UV irradiation is then characterized by Eq. (2), in which the monomer consumption rate is mainly influenced by monomer concentration ($M(x,t)$), a composite kinetic factor (κ), and a distributed control input ($u(x,t)$). The definitions of κ and $u(x,t)$ are given by:

$$\kappa = -\frac{k_p}{k_t^{0.5}}\sqrt{\phi\varepsilon P_0} \tag{4}$$

$$u(x,t) = \exp\left(-\frac{\phi\varepsilon}{2}\cdot\int_0^t I(x,\tau)d\tau\right)\sqrt{I(x,t)} \tag{5}$$

where k_p, k_t denote the propagation and termination rate constants, respectively. P_0 is the initial concentration of the photo-initiator. ϕ and ε represent the quantum yield for initiation and the molar absorptivity, respectively. The thermal evolution associated with the polymerization is described by Eq. (3). The thermal dynamics is governed by reaction heat generation, conductive and convective heat transfer. The radiative heat transfer is ignored here because the temperature of the target is comparatively low. In Eq. (3), ρ and c are averaged density and specific heat capacity of the paint film. ΔH is the polymerization enthalpy. λ, h, and T_∞ denote the conductive and convective heat transfer coefficients, and the ambient temperature, respectively. The polymerization rate R_p is defined as:

$$R_p = -\frac{dM(x,t)}{dt} \tag{6}$$

It can be seen from Eqs. (1) ~ (3) that the UV curing process with a moving actuator is a highly nonlinear, distributed-parameter process. To simplify the control design, the above curing process model is reduced by using a simplified irradiation model and a linearized polymerization model.

Simplification of the Irradiation Model

The actual control input ($u(x,t)$) defined in Eq. (5) is a nonlinear function of the UV irradiation distribution ($I(x,t)$) on the target. The latter is also a nonlinear function of two manipulated variables: the intensity ($\varphi(t)$) and position ($x_a(t)$) of the moving actuator. Since the quantum yield for initiation ϕ is usually very small, $u(x,t)$ is approximately equal to $\sqrt{I(x,t)}$. Therefore, a triangular model with the following definition is used to approximate the actual irradiation model (the absorption coefficient $\eta(x)$ will be integrated later):

$$u(x,t)=0,\quad x\in[0,x_a-w] \text{ or } x\in[x_a+w,L] \tag{7}$$

$$u(x,t)=\left(1+\frac{x}{w}\right)u_m-\frac{u_m}{w}x_a,\quad x\in(x_a-w,x_a) \tag{8}$$

$$u(x,t)=\left(1-\frac{x}{w}\right)u_m+\frac{u_m}{w}x_a,\quad x\in(x_a,x_a+w) \tag{9}$$

Here, u_m and w represent the height and half width of the triangle. x_a denotes the position of the moving actuator. The total length of the target is denoted by L. Fig. 1 illustrates both the actual source model and the triangular model.

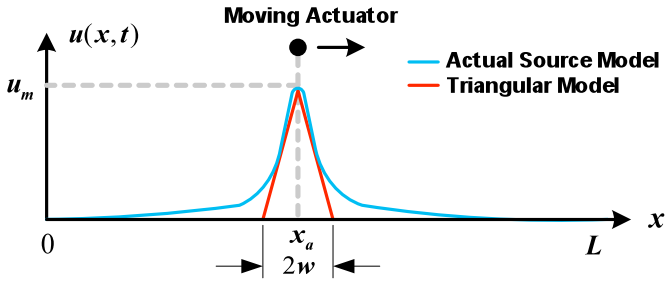

FIGURE 1. THE SIMPLIFIED SOURCE MODEL

Given the assumption that ϕ is very small, u_m can be approximated by:

$$u_m\approx\sqrt{I(x_a,t)}=\sqrt{\varphi(t)/\left(\pi d_0^2\right)} \tag{10}$$

In discrete time, if the previous point ($u_m(k-1)$, $x_a(k-1)$) is available, then by dropping higher order terms in the Taylor expansion of these equations, the increment of the control input $\Delta u(x,i)$ within the neighborhood ($i=k,k+1,\cdots,k+H_p$, H_p denotes the prediction horizon discussed later) can be approximately represented as a function of $\Delta u_m(i)$ and $\Delta x_a(i)$:

$$\Delta u(x,i)=0,\quad x\in[0,x_a-w] \text{ or } x\in[x_a+w,L] \tag{11}$$

$$\Delta u(x,i)=\left(1+\frac{x}{w}-\frac{x_a(k-1)}{w}\right)\Delta u_m(i)-\frac{u_m(k-1)}{w}\Delta x_a(i),\quad x\in(x_a-w,x_a) \tag{12}$$

$$\Delta u(x,i)=\left(1-\frac{x}{w}+\frac{x_a(k-1)}{w}\right)\Delta u_m(i)+\frac{u_m(k-1)}{w}\Delta x_a(i),\quad x\in(x_a,x_a+w) \tag{13}$$

Linearization of the Polymerization Dynamics

The polymerization governed by Eq. (2) is a nonlinear dynamic process involving the controlled variable $M(x,t)$ and the distributed input $u(x,t)$. In discrete time, the first-order Taylor approximation of Eq. (2) can be represented by:

$$\begin{aligned}&\frac{M(x,i+1)-M(x,i)}{dt}\\&=\kappa\left[M(x,k-1)u(x,k-1)+u(x,k-1)\Delta M(x,i)\right.\\&\quad\left.+M(x,k-1)\Delta u(x,i)\right]\\&=\kappa\ u(x,k-1)\left[M(x,k-1)+\Delta M(x,i)\right]\\&\quad+\kappa M(x,k-1)\Delta u(x,i)\\&=\kappa\left[u(x,k-1)M(x,i)+M(x,k-1)\Delta u(x,i)\right]\\&\qquad(i=k,k+1,\cdots,k+H_p)\end{aligned} \tag{14}$$

Here, the previous control input $u(x,k-1)$ and monomer concentration $M(x,k-1)$ are considered as constants at the current sampling period, although both of them will be updated when the next measurement becomes available. $u(x,k-1)$ is provided by the controller, and $M(x,k-1)$ is obtained through an online estimation scheme using a dual extended Kalman filter (DEKF) [13].

The complete discretized polymerization model can be obtained by substituting the input increment $\Delta u(x,i)$ defined by Eqs. (11) ~ (13) into Eq. (14). The discrete state-space form of the complete model is presented as follows:

$$\vec{M}(i+1)=A\vec{M}(i)+B\Delta\vec{U}(i) \tag{15}$$

$$\begin{aligned}&\vec{M}(i)=\left\{M_1(i),M_2(i),\cdots,M_N(i)\right\}^{\mathrm{T}},\\&\Delta\vec{U}(i)=\left\{\Delta u_m(i),\ \Delta x_a(i)\right\}^{\mathrm{T}}\end{aligned} \tag{16}$$

$$A=\underset{j=1,2,\cdots,N}{\mathrm{diag}}\left\{\kappa\ dt\ u_j(k-1)+1\right\},\ B=\begin{bmatrix}b_{11}&b_{12}&\cdots&b_{1N}\\b_{21}&b_{22}&\cdots&b_{2N}\end{bmatrix}^{\mathrm{T}}\quad(i=k,k+1,\cdots,k+H_p) \tag{17}$$

In Eqs. (15) ~ (17), the spatial domain ($[0,L]$) is divided into N units. Here, the vector $\vec{M}(i)$ represents the monomer distribution along $[0,L]$. The input vector $\Delta\vec{U}(k)$ is composed of $\Delta u_m(i)$ and $\Delta x_a(i)$. The time discretization index and the

time step are denoted by k and dt, respectively. $u_j(k-1)$ is calculated by using the triangular model defined by Eqs. (7) ~ (9). The elements of the matrix B are defined as follows:

$$b_{1j} = 0,\ b_{2j} = 0, \quad jL/N \in [0,\ x_a(k-1) - w] \text{ or } jL/N \in [x_a(k-1) + w,\ L] \tag{18}$$

$$b_{1j} = \eta_j M_j(k-1)\left(1 + \frac{jL/N}{w} - \frac{x_a(k-1)}{w}\right),$$

$$b_{2j} = \eta_j M_j(k-1)\left[-\frac{u_m(k-1)}{w}\right], \tag{19}$$

$$jL/N \in (x_a(k-1) - w,\ x_a(k-1))$$

$$b_{1j} = \eta_j M_j(k-1)\left(1 - \frac{jL/N}{w} + \frac{x_a(k-1)}{w}\right),$$

$$b_{2j} = \eta_j M_j(k-1)\left[\frac{u_m(k-1)}{w}\right], \tag{20}$$

$$jL/N \in (x_a(k-1),\ x_a(k-1) + w)$$

$$(j = 1,\ 2,\ \cdots,\ N)$$

where, η_j is the element of the estimated absorption coefficient vector $\vec{\eta}$ (Here, the neglect of $\vec{\eta}$ in developing the triangular source model has been compensated). This linear model defined by Eqs. (15) ~ (20) can be used to predict future states during the current sampling period.

MODEL PREDICTIVE CONTROL

Given the curing model represented by Eqs. (15) ~ (20), the control objective to be addressed is as follows: achieve a desired monomer concentration distribution by adjusting two manipulated variables (intensity and position) of the moving actuator. A model predictive control (MPC) framework can coordinate multiple manipulated variables optimally and handle actuation limitations at the same time [18, 19]. Here, we will detail the development of the MPC formulation for this particular problem using the linear model established in the previous section.

The Basic Control Structure

The basic MPC structure for the UV curing process is illustrated in Fig. 2. In this structure, the MPC controller acquires essential states and parameters from the estimator and generates the optimized control signals (u_m, x_a) for the actual curing process so that the desired curing distribution or quality can be achieved.

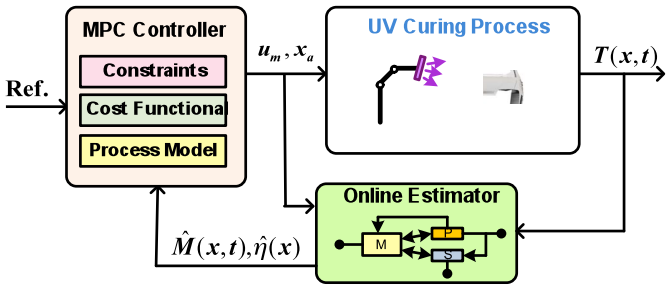

FIGURE 2. THE CONTROL STRUCTURE

Inside the MPC controller, three fundamental elements are considered. First, a process model described by Eq. (15) will be used to predict future states along a pre-defined time horizon. A cost functional regarding both the control performance and energy use is then established to guide the online optimization. In addition, the actuation constraints will be incorporated into the scheme to obtain feasible solutions. The mathematical details of the MPC formulation are given below.

Mathematical Formulation of MPC

The general formulation of MPC based on a linear model has been discussed in [18]. It turns out that the original formulation needs to be changed in order to use it for this particular distributed-parameter problem. Given the linear model described by Eq. (15), the future state (monomer concentration distribution) along the prediction horizon can be obtained by:

$$\begin{aligned}
\vec{M}(k+1) &= A\vec{M}(k) + B\Delta\vec{U}(k \mid k-1) \\
\vec{M}(k+2) &= A\vec{M}(k+1 \mid k) + B\Delta\vec{U}(k+1 \mid k-1) \\
&= A^2\vec{M}(k) + AB\Delta\vec{U}(k \mid k-1) \\
&\quad + B\left[\Delta\vec{U}(k \mid k-1) + \Delta\vec{U}(k+1 \mid k)\right] \\
&= A^2\vec{M}(k) + (A+I)B\Delta\vec{U}(k \mid k-1) \\
&\quad + B\Delta\vec{U}(k+1 \mid k) \\
&\vdots \qquad\qquad \vdots \\
\vec{M}(k+H_u) &= A^{H_u}\vec{M}(k) + \Gamma_0(A,B)\Delta\vec{U}_k^{k+H_u-1} \\
\vec{M}(k+H_u+1) &= A^{H_u+1}\vec{M}(k) + \Gamma_1(A,B)\Delta\vec{U}_k^{k+H_u-1} \\
&\vdots \qquad\qquad \vdots \\
\vec{M}(k+H_p) &= A^{H_p}\vec{M}(k) + \Gamma_q(A,B)\Delta\vec{U}_k^{k+H_u-1}
\end{aligned} \tag{21}$$

$$\begin{aligned}
\Delta\vec{U}_k^{k+H_u-1} = \Big\{&\Delta\vec{U}(k \mid k-1),\ \Delta\vec{U}(k+1 \mid k),\ \cdots \\
&,\ \Delta\vec{U}(k+H_u-1 \mid k+H_u-2)\Big\}^{\mathrm{T}}
\end{aligned} \tag{22}$$

$$\begin{aligned}
\Gamma_0(A,B) &= \left\{\sum_{i=0}^{H_u-1} A^i B,\ \sum_{i=0}^{H_u-2} A^i B,\ \cdots,\ B\right\} \\
\Gamma_1(A,B) &= \left\{\sum_{i=0}^{H_u} A^i B,\ \sum_{i=0}^{H_u-1} A^i B,\ \cdots,\ \sum_{i=0}^{1} A^i B\right\} \\
&\vdots \qquad\qquad \vdots \\
\Gamma_q(A,B) &= \left\{\sum_{i=0}^{H_p-1} A^i B,\ \sum_{i=0}^{H_p-2} A^i B,\ \cdots,\ \sum_{i=0}^{q} A^i B\right\} \\
&\qquad\qquad \left(q = H_p - H_u\right)
\end{aligned} \tag{23}$$

In Eqs. (21) ~ (23), H_p and H_u denotes the prediction and control horizons, respectively. $\Delta\vec{U}_k^{k+H_u-1}$ is a vector composed of the increments of control input along the control horizon H_u. The increment is defined as the difference between the control inputs at two adjacent time steps (e.g. $\Delta\vec{U}(k\,|\,k-1) = \vec{U}(k) - \vec{U}(k-1)$). Beyond the control horizon H_u, the increment of control input is set to zero (e.g. $\Delta\vec{U}(k+H_u\,|\,k+H_u-1) = \vec{0}$). The predicted future states described by Eqs. (21) ~ (23) can also be written in matrix-vector form:

$$\vec{M}_{k+1}^{k+H_p} = \gamma\vec{M}(k) + \xi\,\Delta\vec{U}_k^{k+H_u-1} \tag{24}$$

$$\vec{M}_{k+1}^{k+H_p} = \begin{bmatrix} \vec{M}(k+1) \\ \vec{M}(k+2) \\ \vdots \\ \vec{M}(k+H_u) \\ \vec{M}(k+H_u+1) \\ \vdots \\ \vec{M}(k+H_p) \end{bmatrix},\quad \gamma = \begin{bmatrix} A \\ A^2 \\ \vdots \\ A^{H_u} \\ A^{H_u+1} \\ \vdots \\ A^{H_p} \end{bmatrix} \tag{25}$$

$$\xi = \begin{bmatrix} B & 0 & \cdots & 0 \\ (A+I)B & B & \cdots & 0 \\ \vdots & \vdots & \ddots & \vdots \\ \sum_{i=0}^{H_u-1} A^i B & \sum_{i=0}^{H_u-2} A^i B & \cdots & B \\ \sum_{i=0}^{H_u} A^i B & \sum_{i=0}^{H_u-1} A^i B & \cdots & (A+I)B \\ \vdots & \vdots & \ddots & \vdots \\ \sum_{i=0}^{H_p-1} A^i B & \sum_{i=0}^{H_p-2} A^i B & \cdots & \sum_{i=0}^{H_p-H_u} A^i B \end{bmatrix} \tag{26}$$

The prediction scheme in Eq. (24) shows that the future states $\vec{M}_{k+1}^{k+H_p}$ can be computed from the current state $\vec{M}(k)$ (estimated monomer concentration distribution) and the assumed future input changes $\Delta\vec{U}_k^{k+H_u-1}$. Now the next task is to find an optimal set of $\Delta\vec{U}_k^{k+H_u-1}$ to minimize the following cost functional:

$$\begin{aligned}
V\left(\Delta\vec{U}_k^{k+H_u-1}\right) &= \left(\vec{M}_{k+1}^{k+H_p} - M_0\right)^{\mathrm{T}} Q\left(\vec{M}_{k+1}^{k+H_p} - M_0\right) \\
&\quad + \left(\Delta\vec{U}_k^{k+H_u-1}\right)^{\mathrm{T}} R\left(\Delta\vec{U}_k^{k+H_u-1}\right)
\end{aligned} \tag{27}$$

where M_0 represents the sequence of desired monomer distribution along the prediction horizon. Q is a $(NH_p)\times(NH_p)$ positive semi-definite matrix used to penalize the state error. R is a $(2H_u)\times(2H_u)$ positive definite matrix that penalizes the control cost. N is the number of elements in the state vector $\vec{M}(k)$ representing the distribution of monomer concentration. The cost functional can be reorganized further by substituting Eq. (24) into Eq. (27):

$$\begin{aligned}
V\left(\Delta\vec{U}_k^{k+H_u-1}\right) &= \left(\xi\,\Delta\vec{U}_k^{k+H_u-1} + E\right)^{\mathrm{T}} Q\left(\xi\,\Delta\vec{U}_k^{k+H_u-1} + E\right) \\
&\quad + \left(\Delta\vec{U}_k^{k+H_u-1}\right)^{\mathrm{T}} R\left(\Delta\vec{U}_k^{k+H_u-1}\right) \\
&= G\,\Delta\vec{U}_k^{k+H_u-1} + \left(\Delta\vec{U}_k^{k+H_u-1}\right)^{\mathrm{T}} H\Delta\vec{U}_k^{k+H_u-1} \\
&\quad + E^{\mathrm{T}}QE
\end{aligned} \tag{28}$$

$$E = \gamma\vec{M}(k) - M_0,\ G = 2E^{\mathrm{T}}Q\xi,\ H = \xi^{\mathrm{T}}Q\xi + R \tag{29}$$

Now the optimization objective can be achieved by solving the quadratic programming (QP) problem described by Eqs. (28) and (29). The associated actuation constraints can be represented by:

$$U_{lb} \le U(i) \le U_{ub},\ \Delta U_{lb} \le \Delta U(i\,|\,i-1) \le \Delta U_{ub} \tag{29}$$

$$\begin{aligned}
U(i) &= \left\{u_m(i), x_a(i)\right\}^{\mathrm{T}}, \\
\Delta U(i\,|\,i-1) &= \left\{\Delta u_m(i\,|\,i-1), \Delta x_a(i\,|\,i-1)\right\}^{\mathrm{T}}
\end{aligned} \tag{30}$$

$$i = k,\ k+1,\ \cdots,\ k+H_u-1 \tag{31}$$

The detailed procedure for implementing the MPC formulation follows the following procedure.

1) Estimate the current monomer concentration distribution $\vec{M}(k)$ by using the measurement of the temperature distribution and the estimator described in [13].
2) Update the linear model (update matrices A and B) by using the previous input $\vec{U}(k-1)$ and the current state estimation $\vec{M}(k)$
3) Predict future states (calculate matrices γ and ξ) for the prediction horizon H_p, starting from the current state estimation $\vec{M}(k)$.
4) Solve the constrained QP problem, by first specifying and computing E, G and H and then finding the optimal sequence of $\Delta\vec{U}_k^{k+H_u-1}$ for the control horizon H_u.

5) Add only the first part of the increment ($\Delta\vec{U}(k \mid k-1)$) of the optimal sequence into the previous input $\vec{U}(k-1)$ and then apply the new input to the curing process.

The above procedure will be repeated when the next estimation becomes available.

SIMULATION RESULTS

In this section, a simulation study is conducted to validate the proposed MPC strategy. The complete nonlinear model of the curing process (described by Eqs. (1) ~ (3)) is established in MATLAB/Simulink. The FTCS (Forward-Time Central-Space) method is used to solve the partial differential equation (Eq. (3)) numerically. Another reduced nonlinear model is developed for implementing the state/parameter estimation (detailed in [13]). The MPC controller (including the linearized process model and QP formulation) is also developed in MATLAB/Simulink. The QP problem is solved by using MATLAB Optimization Toolbox [20].

The simulation time step is set to 0.01s for the full nonlinear model. Both the estimator and MPC controller run a little slower (0.05s) than the full model to reduce the computation cost. All the parameters associated with the curing process are obtained from [21]. The rest of this section will discuss the tuning of the MPC controller and the results for different control scenarios.

Tuning of the MPC Controller

To implement the MPC controller, a set of parameters need to be determined, including the prediction and control horizon (H_p and H_u), the weight matrices Q and R, and the constraints on the input and the input increment. The selection of prediction and control horizon is a trade-off between control performance and computation cost. Here, H_p and H_u are set to 8 (8×0.05s) and 6 (6×0.05s), respectively. The weight matrices Q and R influence the balance between the control cost and the state deviation from the reference. Particularly, the Q matrix has two significant characteristics. First, it should largely emphasize or coincide with the dominant irradiance distribution of the source/actuator. Second, it needs to be updated at each calculation period to follow the moving actuator.

In addition, setting constraints also plays a significant role in tuning the MPC controller. Two types of constraints are considered here. First, for the two manipulated variables (u_m and x_a), they should be constrained as: $u_m \in [0,\ u_{\max}]$ and $x_a \in [0,\ L]$. $u_{\max}$ is the upper limit of the UV intensity and L is the spatial boundary of the target. These constrains guarantee that the actuator only moves within the defined scope and applied limited power. Second, there are also some constraints on the change of the control input (Δu_m and Δx_a). These constraints are usually determined by the physical limitations of the actuator (e.g. it cannot move/accelerate too fast).

Demonstration of the MPC Strategy

To demonstrate the proposed MPC strategy, three simulation scenarios are defined as follows: 1) Uniform UV absorption, low set point for cure conversion; 2) Uniform absorption, high set point; 3) Uneven absorption, moderate set point. The corresponding results are illustrated in Figs. 3 ~ 8.

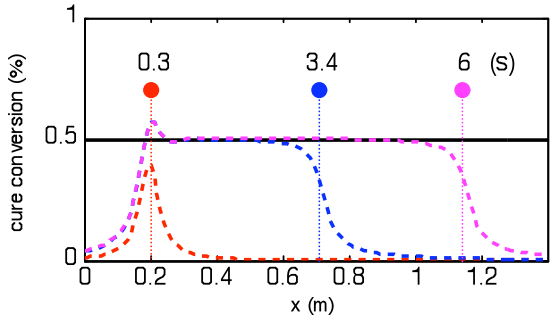

FIGURE 3. CURE CONVERSION DISTRIBUTION AT t=0.3, 3.4, and 6s (UNIFORM ABSORPTION, LOW SET POINT)

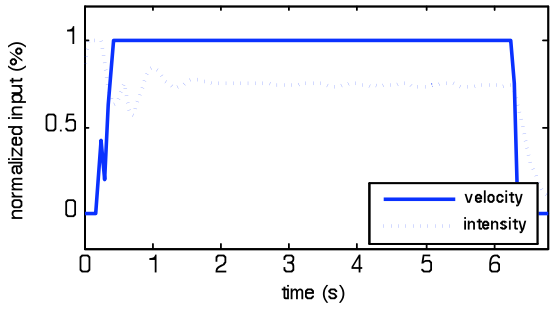

FIGURE 4. TIME HISTORY OF INTENSITY AND VELOCITY (UNIFORM ABSORPTION, LOW SET POINT)

Fig. 3 shows the cure conversion distribution along the target when the moving actuator (depicted by the solid ball) crosses different positions. The reference cure conversion is set to 50% (half-cured). The actuator's position (x) is limited in the range of [0.2, 1.2] (m). Fig. 4 shows the time history of two significant factors of the actuator: intensity and velocity (obtained from the position and known time step). Both of them are normalized with respect to their maximum values. When the actuator starts from the initial position (x = 0.2m), the intensity is set to its maximum value and the velocity stays at zero. This makes the local cure conversion around the initial position increases as fast as possible (illustrated by the red dash line in Fig. 3). Then the actuator's velocity is adjusted to its maximum value quickly and the intensity settles at some level between zero and the maximum value. Once the actuator reaches the

terminal position (x = 1.2m), it will stop there and the intensity is reduced to zero. Overall, for this scenario (uniform absorption, low set point), the MPC controller prefers adjusting the intensity rather than the velocity.

Figs. 5 and 6 illustrate results for the second scenario, in which the UV absorption distribution remains uniform, but the set point of the cure conversion is increased to 80%. In this case, the final cure conversion shown in Fig. 5 still matches the set point well, but the MPC controller runs in a different mode.

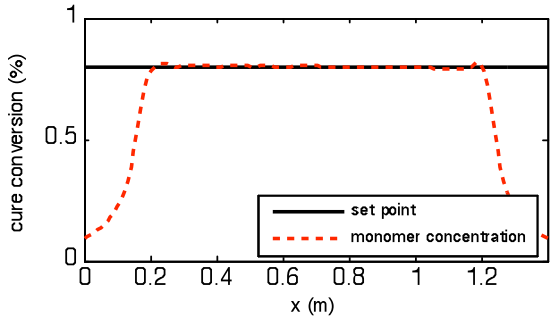

FIGURE 5. FINAL CURE CONVERSION DISTRIBUTION (UNIFORM ABSORPTION, HIGH SET POINT)

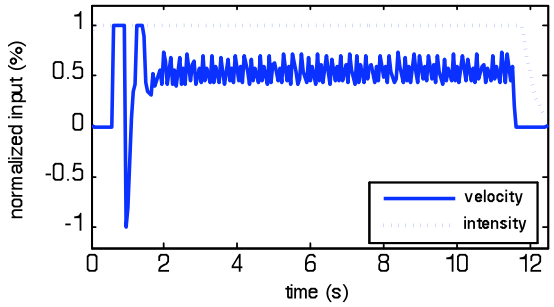

FIGURE 6. TIME HISTORY OF INTENSITY AND VELOCITY (UNIFORM ABSORPTION, HIGH SET POINT)

The time history illustrated in Fig. 6 shows that the intensity always gets saturated during the curing process, while the velocity is regulated to a certain value to ensure the desired cure conversion. The two scenarios above also illustrate how the MPC controller deals with constraints on input (intensity or u_m) and the change of input (velocity or Δx_a).

In the last scenario, uneven UV absorption along the target (depicted by the blue dash-dot line in Fig. 7) is introduced and a moderate set point of cure conversion (60%) is selected. Fig. 7 shows that the MPC controller maintains the cure conversion uniformity at the desired set point, although the UV absorption is uneven. The operation is explained using Fig. 8. When the actuator passes the area with lower UV absorption, the intensity is set to its maximum value and the velocity changes between zero and its maximum value. Once the actuator enters the area with higher UV absorption, the velocity stays at its maximum value and the intensity begins to decrease. This manipulation compensates for the unevenness of UV absorption and helps achieve the desired cure uniformity. Fig. 8 also illustrates how the two operation modes (intensity-based and velocity-based) are combined in this particular case.

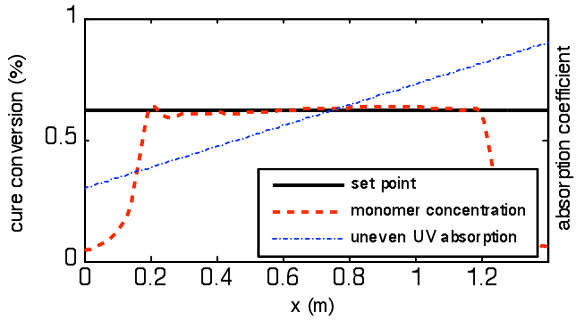

FIGURE 7. FINAL CURE CONVERSION DISTRIBUTION (UNEVEN ABSORPTION, MODERATE SET POINT)

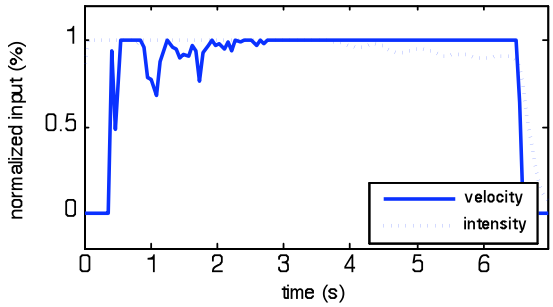

FIGURE 8. TIME HISTORY OF INTENSITY AND VELOCITY (UNEVEN ABSORPTION, MODERATE SET POINT)

In summary, the results for the three scenarios above demonstrate that the proposed MPC controller (with state estimation) is able to manipulate the two key variables (intensity and velocity) within the actuation limitations so that the desired cure level and uniformity can be achieved under either uniform or uneven UV absorption.

CONCLUSIONS

In this paper, a model predictive control strategy has been formulated for a distributed-parameter curing process with a moving radiant actuator. The formulation of the proposed MPC controller is based on spatial and temporal discretization of the linearized curing process model and a previously developed online state/parameter estimator. A triangular source model is also established to approximate the distribution of the actuator input (irradiation) in the curing process. The process model is then utilized to design the MPC strategy, in which the intensity and velocity (position) of the actuator is optimally manipulated based on the updated state/parameter estimation, the selected cost functional and physical actuation constraints. A simulation study has been conducted to demonstrate the proposed control

strategy. The results show that the proposed MPC strategy works well in maintaining the desired cure level and uniformity, even in the existence of disturbance (e.g., unevenness in UV absorption).

Future work in this area will expand the MPC scheme to other similar processes that use moving radiant actuators (e.g. painting, drying, etc.) and establish a more general framework to guide the control design for these processes.

REFERENCES

[1] Hagood, D. and Kelly, M., 2008. "Extolling the Advantages of UV-Curing Processes". *Metal Finishing*, 106(4), April, pp. 71-74.

[2] Dhib, R., 2007. "Infrared Drying: from Process Modeling to Advanced Process Control". *Drying Technology*, 25(1), January, pp. 97-105.

[3] Joesel, K., 2005. "Process Solutions for UV Curing of Coatings on Automotive Plastic Parts". In RadTech Europe 2005 Conference Papers Archive, See also URL: http://www.radtech-europe.com/files_content/joeselpapernovember2006.pdf

[4] Raith, T., Bischof, M., Deger, M., and Gemmler, E., 2001. "3-D UV Technology for OEM Coatings". In RadTech Europe 2001 Conference Papers Archive, See also URL: http://www.radtech-europe.com/files_content/raithpapernovember.pdf

[5] Mills, P., 2006. "Robotic UV Curing Saves Time and Money". *Metal Finishing*, 104(4), April, pp. 43-49.

[6] Butkovskiy, A. G. and Pustyl'Nikov, E. I., 1980. "Theory of Mobile Control of Distributed Parameter Systems". *Automation and Remote Control*, 41(6), June, pp. 741-747.

[7] Vayena, O., Doumanidis, H., Demetriou, M. A., 2000. "An LQR-based Optimal Actuator Guidance in Thermal Processing of Materials". In Proceedings of the 2000 American Control Conference, Chicago, IL, USA, pp. 2300-2304.

[8] Demetriou, M.A., Paskaleva, A., Vayena, O., Doumanidis, H., 2003. "Scanning Actuator Guidance Scheme in a 1-D Thermal Manufacturing Process". *IEEE Transactions on Control Systems Technology*, 11(5), September, pp. 757-764.

[9] Demetriou, M.A., 2008. "Guidance of a Moving Collocated Actuator/Sensor for Improved Control of Distributed Parameter Systems". In Proceedings of the 47th IEEE Conference on Decision and Control, pp. 215-220.

[10] Jones, P.D.A., Duncan, S.R., Rayment, T., Grant, P.S., 2003. "Control of Temperature Profile for a Spray Deposition Process". *IEEE Transactions on Control Systems Technology*, 11(5), September, pp. 656-667.

[11] Zeng, F., Ayalew, B., Omar, M., 2009. "Robotic Automotive Paint Curing Using Thermal Signature Feedback", I*ndustrial Robot: An International Journal*, 36(4), pp. 389-395.

[12] Zeng, F., Ayalew, B., Omar, M., 2009. "Control of a Robotic UV Curing Process with Thermal Vision Feedback through Two IR Cameras", In Proceedings of the 2009 ASME International Mechanical Engineering Congress & Exposition, Lake Buena Vista, FL, USA (In Press).

[13] Zeng, F., Ayalew, B., 2010, "Online Distributed State and Parameter Estimation for Feedback Control of a Curing Process". In Proceedings of the 2010 American Control Conference, Baltimore, MD, USA (Accepted).

[14] Dufour, P., Toure, Y., Blanc, D., Laurent, P., 2003. "On Nonlinear Distributed Parameter Model Predictive Control Strategy: On-line Calculation Time Reduction and Application to an Experimental Drying Process". *Computers & Chemical Engineering*, 27(11), November, pp. 1533-1542.

[15] Bombard, I., Da Silva, B., Dufour, P., Laurent, P., 2010. "Experimental Predictive Control of the Infrared Cure of a Powder Coating: A Non-linear Distributed Parameter Model Based Approach". *Chemical Engineering Science*, 65(2), pp. 962-975.

[16] Dubljevic, S., El-Farra, N.H., Mhaskar, P., Christofides, P.D., 2006. "Predictive Control of Parabolic PDEs with State and Control Constraints". *International Journal of Robust and Nonlinear Control*, 16(16), November, pp. 749-772.

[17] Decker, C., 1996. "Photoinitiated Crosslinking Polymerization". Progress in Polymer Science (Oxford), 21(4), pp. 593-650.

[18] Maciejowski, J. M., 2002. Prediction Control: with Constraints. Prentice Hall, Upper Saddle River, NJ, USA.

[19] Rawlings, J. B., 1999. "Tutorial: Model Predictive Control Technology". In Proceedings of the 1999 American Control Conference, vol.1, pp. 662-676.

[20] The Mathworks, Inc., User's Guide to Optimization Toolbox, URL: http://www.mathworks.com/access/helpdesk/help/toolbox/optim/ug/bqartsw.html

[21] Hong, W., Lee, Y. T., Gong, H., 2004. "Thermal Analysis of Layer formation in a Stepless Rapid Prototyping Process", Applied Thermal Engineering, 24(2-3), February, pp. 255-268.